NIST Technical Note 2064

OpenSC – an Open-source Calculation Tool for Combustion Mixture Emissivity/Absorptivity

Wai Cheong Tam
Walter W. Yuen

This publication is available free of charge from:
http://dx.doi.org/10.6028/NIST.TN.2064

National Institute of Standards and Technology
U.S. Department of Commerce

NIST Technical Note 2064

OpenSC – an Open-source Calculation Tool for Combustion Mixture Emissivity/Absorptivity

Wai Cheong Tam
Fire Research Division
Engineering Laboratory
National Institute of Standards and Technology
Gaithersburg, MD 20899

Walter W. Yuen
Department of Mechanical Engineering
Santa Clara University
Santa Clara, CA 95053

June 2019

U.S. Department of Commerce
Wilbur L. Ross, Jr., Secretary

National Institute of Standards and Technology
Walter Copan, NIST Director and Under Secretary of Commerce for Standards and Technology

National Institute of Standards and Technology Technical Note 2064

Natl. Inst. Stand. Technol. Tech. Note 2064, 28 pages (Jun. 2019)

CODEN: NTNOEF

This publication is available free of charge from:

https://doi.org/10.6028/NIST.TN.2064

OpenSC – an Open-source Calculation Tool for Combustion Mixture Emissivity/Absorptivity

ABSTRACT

A web-based radiation code, OpenSC, is developed to provide an ease-of-use calculation tool to evaluate total emissivity and total absorptivity of a typical combustion mixture consisting of H_2O, CO_2, N_2, O_2, and/or soot particulates. The web-based calculation tool utilizes the mathematical formulation of a neural network-based correlation (RAD-NNET) and accounts for the realistic emission/absorption effect of non-gray gases and soot particulates.

A set of examples is provided to illustrate the use of OpenSC to determine the total emissivity and total absorptivity for $H_2O/CO_2/N_2$/soot mixture in various conditions. Commonly accepted approximate approaches used in fire safety/protection design calculations for the evaluation of non-gray effects for radiation heat transfer, as recommended by engineering handbooks, are assessed. In comparison to results generated by OpenSC, error associated with the predictions obtained from using the approximate approaches is substantial. Quantitative comparison also demonstrates that the gray assumption with the total emissivity equal to the total absorptivity is generally invalid. The emissivity chart method, an approach which has been accepted by many practicing engineers in the fire safety community, can lead to substantial error.

KEYWORDS: Neural network, radiative properties, non-gray, total emissivity chart.

Disclaimer

This software was developed at the National Institute of Standards and Technology by employees of the Federal Government in the course of their official duties. Pursuant to title 17 Section 105 of the United States Code this software is not subject to copyright protection and is in the public domain. This calculation tool is an experimental system. NIST assumes no responsibility whatsoever for their use by other parties, and makes no guarantees, expressed or implied, about their quality, reliability, or any other characteristic. We would appreciate acknowledgement if the software is used. This software can be redistributed and/or modified freely provided that any derivative works bear some notice that they are derived from it, and any modified versions bear some notice that they have been modified.

Table of Contents

This page intentionally left blank.

1. INTRODUCTION

The radiative transfer equation (RTE) that governs the propagation of radiation through an absorbing and emitting medium is a multi-dimensional partial differential equation with spectral dependence properties. Solving such an equation is exceedingly difficult and the numerical complexity is exacerbated by the strongly spectral dependence of the radiative properties of non-gray gases, such as H_2O and CO_2 [1]. For example, the absorption coefficient of water vapor in the 6.3 μm band with a gas temperature at 1000 K and total pressure of 1 atm is shown in Fig. 1. The spectral behavior of H_2O is highly irregular and is described by more than ten thousand lines. Detailed spectral evaluation accounting for different line structures is typically required to evaluate the total emissivity/absorptivity. In addition to gaseous species, particulates such as soot, coal particles, and aerosols also exist in various practical engineering problems. Even though soot particulates in fire applications are generally expected to be small so that the scattering effect can be neglected [2], the absorption behavior of soot is still a strong function of wavelength. Indeed, an accurate radiation calculation accounting for the effect of non-gray gases and soot particulates is numerically challenging.

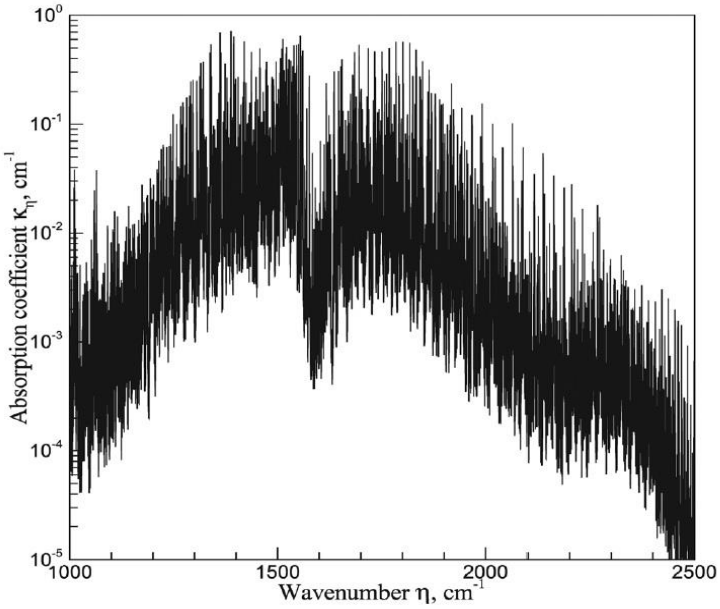

Fig 1. Local absorption coefficient for the 6.3 μm band of H_2O with gas temperature at 1000 K and total pressure at 100 kPa [1].

Over the past 30 years, a significant amount of research has been conducted for the development of computational techniques to evaluate the radiation effect of non-gray gases. It is generally agreed that the Line-by-Line (LBL) method [3] provides the most accurate prediction for the spectral properties of non-gray gases. However, this method requires high-resolution spectroscopic databases and lengthy computational time [4]. Even with today's powerful computers, the LBL method can only be used to generate benchmark solutions. In order to overcome the numerical bottleneck for practical engineering applications, approximate methods such as narrow band models [5], gray gas models [6], and total

emissivity chart models [7] have been developed[1]. Narrow band models (NB) provide predictions for the average spectral absorption coefficient around a narrow band. The results generally agree well with those generated from the LBL models. However, the NB results must still be integrated over the entire spectrum to generate the total emissivity/absorptivity. The direct use of NB models in today's engineering calculations (i.e., fire dynamics simulator [8]) is, therefore, still limited and additional mathematical simplification is required. Gray gas models are more computationally efficient. It assumes that the spectral behavior of a non-gray gas (i.e., H_2O and CO_2) over the entire spectrum can be described by an "equivalent" gray absorption coefficient. However, Edwards [9] pointed out in his studies that treating gas absorption coefficients as gray in high temperature applications can lead to temperature under-predictions of 375 K or more. The gray models often require an extensive database for the "equivalent" gray absorption coefficients. The model also leads to the prediction that the total emissivity and total absorptivity are identical, which is physically incorrect. Therefore, the use of gray gas models is generally not recommended if modeling accuracy is of interest. Total emissivity chart models are established on the basis of experimental measurements. Total (spectrally integrated) emissivity data, at various path-lengths, species concentrations, and temperatures, are typically formulated into empirical charts/correlations. Since the data are obtained for one absorbing gas species, the emissivity chart models are directly applicable only to mixtures with one absorbing gas species (i.e., pure H_2O/N_2 or pure CO_2/N_2 mixture). Ad-hoc empirical approaches are proposed to extend the emissivity chart data for the evaluation of total emissivity for mixture with two absorbing gases and soot, as well as the total absorptivity of a mixture. However, the accuracy of these extensions is highly uncertain as they have not been benchmarked against exact solution. Indeed, as it was demonstrated in recent studies [10-13], these extensions can lead to substantial errors (higher than 100 % or up to 1000 %). Despite the uncertainty associated with the prediction accuracy, the use of empirical charts/correlations and the ad-hoc extensions for the evaluation of the total emissivity/absorptivity for non-gray gases continues. In fact, these charts remain the only information for combustion radiative properties in virtually all fire protection engineering and heat transfer handbooks [14,15]. Indeed, the lack of a simple-to-use and mathematically validated methodology which would allow non-radiation experts to implement the correct physics of radiative transfer into practical engineering design calculations is a serious obstacle, particularly to the fire protection community, in understanding the effect of radiative heat transfer for fire safety consideration.

In this technical note, OpenSC, an Open-source Spectral Calculation tool is developed to simulate the total emissivity/absorptivity of a one-dimensional homogeneous isothermal non-gray medium consisting of typical combustion products (H_2O, CO_2, N_2, O_2, and soot particulates) at one atmosphere (the expected total pressure in most fire safety scenarios). Fundamentally, the calculation algorithms and the neural network correlations used in OpenSC are identical to RAD-NNET[2] (RADiation with Neural NETwork) except that OpenSC is written in a server-side scripting language (PHP - Personal Home Page) whereas RAD-NNET is written in Fortran 90. The primary advantage of using PHP is that the radiation calculation tool can readily be used where there is internet access. In addition, users do not need to have any sophisticated computer hardware, expensive compilers, and extensive knowledge in both programming

[1] Other spectral models include wide-band models [16], k-distributions models [17], and weighted sum of gray gases models [18].

[2] RAD-NNET [13] is a neural network-based correlation for the determination of total emissivity/absorptivity for mixture consisted of H_2O, CO_2, and/or soot particulates.

and radiation heat transfer to carry out complex and detailed radiation calculations, which typically involves more than 15 thousand lines of code, for the evaluation of mixture radiative properties.

The remaining parts of this paper are organized as follow. In section 2, the mathematical formulation associated with the neural networks used in OpenSC is presented. Examples and modeling guidelines for using OpenSC for the determination of total emissivity/absorptivity for various combustion conditions are provided in Section 3. Finally, an assessment of the emissivity chart approach and its ad-hoc extension as currently suggested in the SFPE Fire Protection Engineering Handbook [14] and Handbook of Heat Transfer Fundamentals [15] for the evaluation of total emissivity/absorptivity with mixture consisted of H_2O, CO_2, N_2, and/or soot particulates is presented.

2. MATHEMATICAL FORMULATION

2.1 Absorptivity

This section presents the mathematical formulation for the total absorptivity. Consider a one-dimensional homogeneous mixture consisting of H_2O, CO_2, N_2, and/or soot particulates, the total absorptivity, α, is given by

$$\alpha\left(T_w, T_g, P_{H_2O}, P_{CO_2}, f_v, L\right) = \frac{\int_0^\infty e_{\lambda b}(T_w)\left(1 - e^{-a_\lambda(T_g, P_{H_2O}, P_{CO_2}, f_v)L}\right)d\lambda}{\sigma T_w^4} \tag{1}$$

where T_w is the source temperature, T_g is the gas temperature, P_{H_2O} is the partial pressure of water vapor (H_2O), and P_{CO_2} is the partial pressure of carbon dioxide (CO_2). It should be noted that when the source temperature is the gas temperature ($T_w = T_g$, meaning the gas medium itself is emitting), the above expression can also be used to determine the total emissivity of the mixture. Since the mathematical formulation for the total emissivity is similar to the total absorptivity, the description associated with the mathematical formulation of total emissivity will not be presented to avoid redundancy.

Focusing on applications for typical combustion phenomena (i.e., fires) occurring in atmospheric conditions, the total gas pressure consisted of nitrogen[3] (N_2), H_2O, and CO_2 is assumed to be 101.325 kPa. In Eqn. (1), f_v is the soot volume fraction, L is the physical path-length of the mixture, $e_{\lambda b}(T_w)$ is the blackbody emissive power evaluated at the source temperature (T_w), σ is the Stefan-Boltzmann constant, and a_λ is the local absorption coefficient of the mixture. The mixture absorption coefficient is the sum of two components: a soot component ($\alpha_{\lambda s}$) and a gas component ($\alpha_{\lambda g}$)

$$a_\lambda\left(T_g, P_{H_2O}, P_{CO_2}, f_v\right) = a_{\lambda s}(f_v) + a_{\lambda g}\left(T_g, P_{H_2O}, P_{CO_2}\right) \tag{2}$$

Assuming non-scattering media with an albedo of zero and that the soot particulates satisfy the Rayleigh small-particle limit [19] where the size parameter of the soot $\pi d/\lambda$ is much smaller than unity (with d being the effective diameter of the soot particle and λ is the wavelength), the soot absorption coefficient is given by [20]

[3] Nitrogen and oxygen are treated as transparent to thermal radiation.

$$a_{\lambda s}(f_v) = \frac{c}{\lambda} \tag{3}$$

with

$$c = 36\pi f_v \frac{nk}{(n^2+k^2+2)^2 + 4n^2k^2} \tag{4}$$

where n and k are the real and imaginary part of the soot's index of refraction, respectively. Based on [13], the value associated with n is taken to be 1.6 and k is taken to be 0.5 in the current work. These indices are typically used in fire/combustion calculation [21] and they are applicable for hydrocarbon fuels such as propane soot with atomic hydrogen to carbon ratio of 1/4.6 [22].

The absorption coefficients of gaseous species are obtained using RADCAL [5], a narrow band-based computer code known to have the capability to generate accurate numerical prediction of the radiative properties accounting for the non-gray and overlapping effect of various gaseous species (i.e., H_2O, CO_2, CO, and CH_4). The descriptions associated with models used in RADCAL for the evaluation of the gas absorption coefficients at different energy levels will not be presented here as they are out of the scope of this paper. These details can be readily obtained from the monographs by Grosshandler [5] and Lecoustre [23]. Model validation for RADCAL had been carried out in [13] and the relative error is less than 5 % over the range of the total absorptivity/emissivity from 0.01 to 1. Since OpenSC calculates the total radiative properties using data from RADCAL, it is reasonable to expect that OpenSC has the same degree of numerical accuracy as RADCAL.

In the development of neural network, there is no specific restriction on the selection of data set (i.e., the actual size of the data and the number of input and output variables) other than that they are statistically sufficient to cover the range of interest for the relevant physics. However, the development of the correlation can be done more efficiently if physical considerations are used to select the appropriate set of input and output parameters. Physically, it is well known that the total absorptivity of a gas is mainly a function of the optical thicknesses, ($P_{H_2O}L$ and $P_{CO_2}L$), and soot concentration thickness, f_vL, and does not depend on the physical path-length, L. Since the size of the soot particulates are considered to be sufficiently small such that the Rayleigh small-particle limit of absorption efficient can be satisfied, the soot absorptivity as shown in Eq. (3) can be readily integrated to yield the following closed-form expression [24]

$$\alpha_s(T_w, f_vL) = 1 - \frac{15}{\pi^4}\,\psi^{(3)}\left(1 + \frac{cT_wL}{C_2}\right) \tag{5}$$

where $\psi^{(3)}$ is the pentagamma function for which the tabulated values are provided in Appendix A. In Eq. (5), C_2 is the second radiation constant and the parameter c is a product of the soot volume fraction and the soot optical properties (refer to Eq. (4)). Since the effect of soot absorptivity can now be readily evaluated through a simple algebraic expression in which direct numerical integration is no longer needed, it will be more numerical efficient to obtain a neural network correlation only for the "excess absorptivity", $\Delta\alpha$, given by

$$\Delta\alpha\left(T_w, T_g, P_{H_2O}L, P_{CO_2}L, f_vL\right) = \alpha\left(T_w, T_g, P_{H_2O}L, P_{CO_2}L, f_vL\right) - \alpha_s(T_w, f_vL) \tag{6}$$

The effect of the soot concentration on $\Delta\alpha$ is expected to be minor since the soot concentration effect is already accounted by the soot absorptivity. The neural network correlation is being generated for the excess absorptivity over a wide range of mixture conditions. Discussion associated with the neural network correlations implemented in OpenSC will be provided in the next section. It should be noted that since the total absorptivity, α, cannot be linearly decoupled into a gas component and a soot component, the excess absorptivity, $\Delta\alpha$, is still a function of five independent variables including the soot concentration thickness ($f_v L$). The excess absorptivity becomes the total gas absorptivity in the limit of zero soot volume fractions.

2.2 Neural Network Correlations

This section highlights the neural network correlations utilized in OpenSC. Detailed explanation can be obtained from [13]. As shown in Fig. 2, a three-layer network is used as the structure of the neural network correlations for the evaluation of excess absorptivity. Mathematically, it can be rigorously proved that with an appropriate layer structure and sufficient number of neurons, a neural network can handle any mathematical functions to a high degree of accuracy without any restrictions on the number of independent and dependent variables. The selection of a three-layer network is based on the practical need to maintain the number of neurons required to develop accurate correlations to a reasonable value (i.e., less than 20) while maintaining the desired numerical efficiency. It was shown in [13] that the three-layer structure is adequate to simulate the complex behaviors of the absorptivity data for a wide range of mixture conditions. It should be noted that OpenSC is not a predictive neural network. It is developed to efficiently and accurately retrieve pre-calculated total emissivity/absorptivity data for applications in practical engineering calculations. OpenSC should not be used to predict new radiative absorption and/or emission information outside the range of the RADCAL database on which the neural network is developed. If needed, OpenSC can be readily extended to regions outside of the range presented in this work by additional calculations.

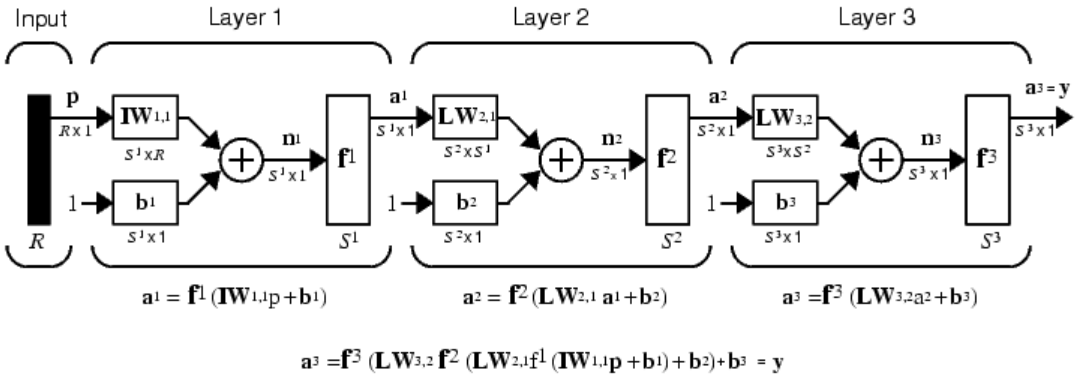

Fig. 2. Structure of a three-layer neural network correlation for the excess absorptivity, $\Delta\alpha\left(T_w, T_g, P_{H_2O}L, P_{CO_2}L, f_v L\right)$ [13].

In Fig. 2, the four distinct layers in the three-layer neural network is presented. The first layer on the left-hand side is the input layer and there are five independent variables including the source temperature (T_w), gas temperature (T_g), total optical thickness of absorptive gaseous species ($P_g L$), absorptive mole fraction of CO_2 (X_{CO_2}), and the soot concentration thickness ($f_v L$). In OpenSC, the absorptive gaseous

species are H_2O and CO_2. The total absorptive gas pressure is the sum of the partial pressure of H_2O, P_{H_2O}, and partial pressure of CO_2, P_{CO_2}, which is written as

$$P_g = P_{H_2O} + P_{CO_2} \tag{7}$$

and the absorptive mole fraction of CO_2 is given by

$$X_{CO_2} = \frac{P_{CO_2}}{P_{H_2O} + P_{CO_2}} \tag{8}$$

Substituting Eq. (7) and (8) into Eq. (6), the excess absorptivity can be rewritten as

$$\Delta\alpha\left(T_w, T_g, P_g L, X_{CO_2}, f_v L\right) = \alpha\left(T_w, T_g, P_g L, X_{CO_2}, f_v L\right) - \alpha_s(T_w, f_v L) \tag{9}$$

The total absorptivity data are generated based on a set of over 19 million data points, corresponding to 550 discrete values of $P_g L$, 11 discrete values of X_{CO_2}, 10 discrete values of $f_v L$, and 18 discrete values of T_w and T_g, respectively. The data set covers the following range of input variables

$$\begin{gathered} 300 \text{ K} \le T_w, T_g \le 2000 \text{ K} \\ 0 \le P_g L \le 2000 \text{ kPa-m} \\ 0 \le X_{CO_2} \le 1.0 \\ 0 \le f_v L \le 10^{-6} \text{ m} \end{gathered} \tag{10}$$

For current applications, the validation shows that the current number of data points and the distribution for the range of input variables are sufficient to formulate an accurate neural network. It should be noted that the existing neural network can be 1) readily updated with the inclusion of new experimental or computational data, 2) expanded to account for other combustion species (i.e., CO, CH_4 and other hydrocarbon fuels), and 3) improved using a more sophisticated spectral model in addition to RADCAL (i.e., the LBL method). These efforts are currently under consideration.

The second layer and the third layer are the hidden layers and the layer on the far-right is the output layer. A hyperbolic tangent sigmoid function is used as the transfer function for the second and the third layer while a linear transfer function is used for the output layer. In OpenSC, the output vector is a scalar (absorptivity) and therefore $S^{(3)}$ is equal to 1. For a given normalized input vector, $\bar{p}_j$, the normalized predicted value of the output, $a^{(3)}$, can be obtained from the following mathematical relations

$$a^{(3)} = \sum_{i=1}^{S^{(2)}} \bar{W}_i^{(3)} \bar{a}_i^{(2)} + b^{(3)} \tag{11}$$

with

$$\bar{a}_i^{(2)} = \tanh\left[\left(\sum_{j=1}^{S^{(1)}} \bar{W}_{ij}^{(2)} \bar{a}_j^{(1)}\right) + \bar{b}_i^{(2)}\right], \qquad i = 1, \ldots, S^{(2)} \tag{12}$$

$$\bar{a}_i^{(1)} = \tanh\left[\left(\sum_{j=1}^{N} \bar{W}_{ij}^{(1)} \bar{p}_j\right) + \bar{b}_i^{(1)}\right], \qquad i = 1, \ldots, S^{(1)} \tag{13}$$

where N being the dimension of the input vector and $a, S, W,$ and b is the output vectors, number of neurons, weight matrices, and the bias vectors, respectively. The superscript associated with $a, S, W,$ and b denotes the actual layer number associated with the three-layer neural network. The three weight matrices $\bar{W}^{(1)}$, $\bar{W}^{(2)}$, and $\bar{W}^{(3)}$ and three bias vectors $\bar{b}^{(1)}$, $\bar{b}^{(2)}$, and $b^{(3)}$ are obtained by the training processes through the neural network development. Readers seeking for details of the training process and the data engineering for the selection of input variables shown in Eq. (10) can refer to [13]. For reference, a set of neural network elements associated with a selected range of mixture conditions is included in Appendix B and one can use the neural network to evaluate radiative properties for the given range of mixture conditions. The rest of the neural network element is available upon request.

3. RESULTS AND DISCUSSION

3.1 Evaluation of Radiative Properties

To demonstrate the operational procedure of OpenSC, the total emissivity/absorptivity for various mixture conditions is determined in this section. Fig. 3a shows the user interface for OpenSC and there are two options for the radiation calculations. For given mixture conditions, which includes a source temperature (T_w), a gas temperature (T_g), a total absorptive optical thickness ($P_g L$), an absorptive mole fraction of CO_2 (X_{CO_2}), and a soot concentration thickness ($f_v L$), the total emissivity/absorptivity can be obtained from a single-value calculation. It should be noted that even though the path-length L is not required as an input parameter, the user is asked to provide a value for L. This input is to remind the user that the absorptive optical thickness divided by the path-length does not exceed 1 atm (~100 kPa). Otherwise, there will be errors and the calculation will not be able to start. For single-value calculations, the computation is efficient and results can be obtained in less than a fraction of a second.

Fill in Input Values: Total Pressure = 1 atm (101 kPa)

Mixture Properties	Single Value Calculation		Range Calculation			
	Select	Value	Select	Minimum Value	Maximum Value	Number of Steps (>=2)
Soot Volume Fraction Pathlength (m): 0 to 0.000001	◉		○			
Temperature (K): 300 to 2000	◉		○			
$CO_2/(CO_2+H_2O)$ Mole Fraction: 0.0 to 1.0	◉		○			
Pressure Pathlength (kPa-m): 0 to 2000 (< Path Length x 1 atm)	◉		○			
Path Length (m): > 0	◉		○			
Source Temperature (K): 300 to 1500	◉		○			

Calculate

Download Results to File

Fig. 3a. User interface of OpenSC.

Fill in Input Values: Total Pressure = 1 atm (101 kPa)

Mixture Properties	Single Value Calculation		Range Calculation			
	Select	Value	Select	Minimum Value	Maximum Value	Number of Steps (>=2)
Soot Volume Fraction Pathlength (m): 0 to 0.000001	◉	0	○			
Temperature (K): 300 to 2000	○		◉	300	2000	18
$CO_2/(CO_2+H_2O)$ Mole Fraction: 0.0 to 1.0	◉	0	○			
Pressure Pathlength (kPa-m): 0 to 2000 (< Path Length x 1 atm)	◉	44.81	○			
Path Length (m): > 0	◉	1	○			
Source Temperature (K): 300 to 1500	◉	300	○			

Calculate

Download Results to File

Fig. 3b. Inputs for the evaluation of pure H_2O emissivity at different gas temperature (since the optical thickness is not evenly distributed, manual input is needed to handle calculations for 10 different optical thicknesses).

The second option is a range calculation. The range calculation offers a capability to carry out parametric studies to understand the effect for different mixture conditions. An example for the determination of total emissivity for pure H_2O at different gas temperature is provided in Fig. 3b. Since the total emissivity of H_2O is of interest in this example, soot volume fraction and absorptive mole fraction of CO_2 are set to be zero. Source temperature is set to be the same as the gas temperature. By clicking the *Calculate* button, the calculation will execute and results for total emissivity will be displayed in the user interface. In order to facilitate further analysis on the radiative properties, the results obtained from either single-value or range calculation can be saved in an Excel spreadsheet by simply clicking the *Download Results to File* button. Generally, input parameters such as partial pressure for gaseous species and volume fraction of soot are not typically being obtained directly from fire design/protection engineering calculations. Therefore, a simple algorithm is included in Appendix C to provide the relevant expressions for the conversion of species/soot mass into appropriate variables with correct units.

3.1.1 Emissivity

A total emissivity chart for pure H_2O generated by OpenSC is presented in Fig. 4 for different optical thicknesses and with gas temperature ranging from 300 K to 2000 K. The relevant inputs for generating the numerical data for a specific absorptive optical thickness are provided in above (refer to Fig. 3b). In Fig. 4, it can be noticed that the total emissivity is a monotonic decreasing function of increasing gas temperature for small optical thickness. When the optical thickness becomes larger, the total emissivity first increases with increasing gas temperature in low temperature region and then decreases from its peak value with increasing gas temperature. The physical mechanism corresponding to the increase or decrease for the total emissivity can be attributed to the unique absorption characteristics associated with H_2O at a specified gas temperature and pressure.

A total emissivity chart for pure CO_2 and the relevant input file for a specific absorptive optical thickness are presented in Fig. 5a and 5b, respectively. The total emissivity of CO_2 is plotted for different absorptive optical thicknesses with gas temperature ranging from 300 K to 2000 K. The slight

nonlinearity in the region of 700 K corresponds to the effect of the strong CO_2 absorption band at 4.3 μm. In comparison to the results shown in Fig. 4, the CO_2 emissivity is lower than the H_2O emissivity and this is generally due to the weaker CO_2 absorption bands.

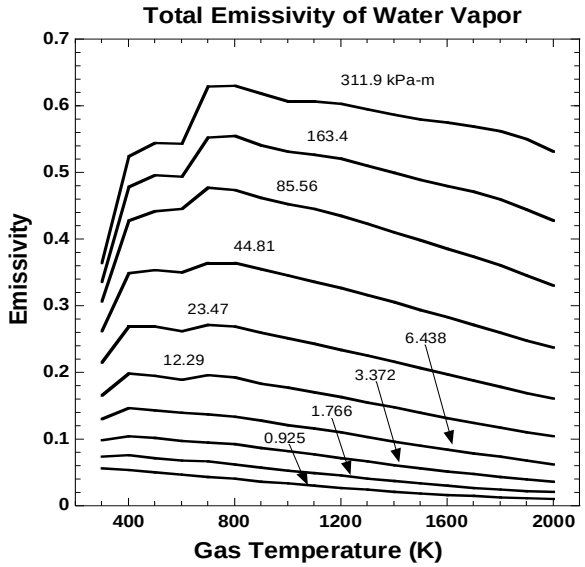

Fig. 4. Calculated total emissivity of H_2O using OpenSC.

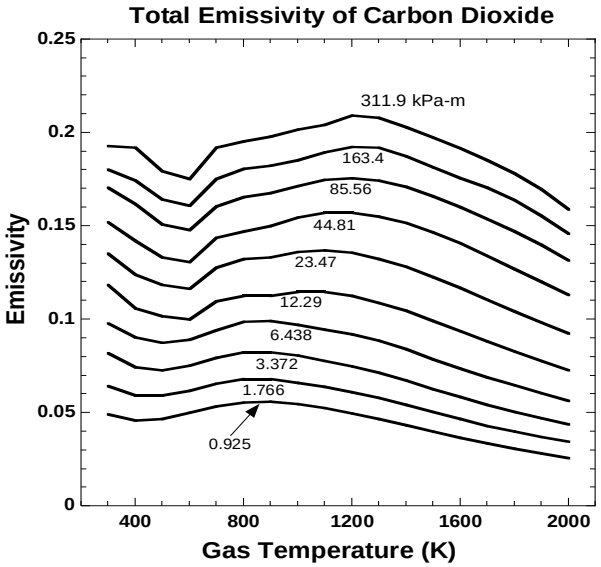

Fig. 5a. Calculated total emissivity of CO_2 using OpenSC.

A total emissivity chart for pure soot is shown in Fig. 6a and the relevant input file is shown in Fig. 6b. The soot emissivity is plotted for different soot concentration thicknesses, f_vL, ranging from 10^{-9} m to 10^{-6} m for a wide range of gas temperature. As shown in the Fig. 6a, in contrast to the emissivity behavior of pure H_2O and pure CO_2, soot emissivity is a monotonic increasing function of increasing gas temperature and this is because of the inverse wavelength dependence of the soot's absorption coefficient. A high emissivity can thus be obtained with either larger value of soot concentration or larger gas temperature. As expected, when the soot concentration is high (i.e., $f_vL > 10^{-6}$ m), the soot emissivity approaches unity.

Fill in Input Values: Total Pressure = 1 atm (101 kPa)

Mixture Properties	Single Value Calculation		Range Calculation			
	Select	Value	Select	Minimum Value	Maximum Value	Number of Steps (>=2)
Soot Volume Fraction Pathlength (m): 0 to 0.000001	◉	0	○			
Temperature (K): 300 to 2000	○		◉	300	2000	18
$CO_2/(CO_2+H_2O)$ Mole Fraction: 0.0 to 1.0	◉	1	○			
Pressure Pathlength (kPa-m): 0 to 2000 (< Path Length x 1 atm)	◉	44.81	○			
Path Length (m): > 0	◉	1	○			
Source Temperature (K): 300 to 1500	◉	300	○			

Calculate

Download Results to File

Fig. 5b. Inputs for the evaluation of pure CO_2 emissivity at different gas temperature (since the optical thickness is not evenly distributed, manual input is needed to handle calculations for 10 different optical thicknesses).

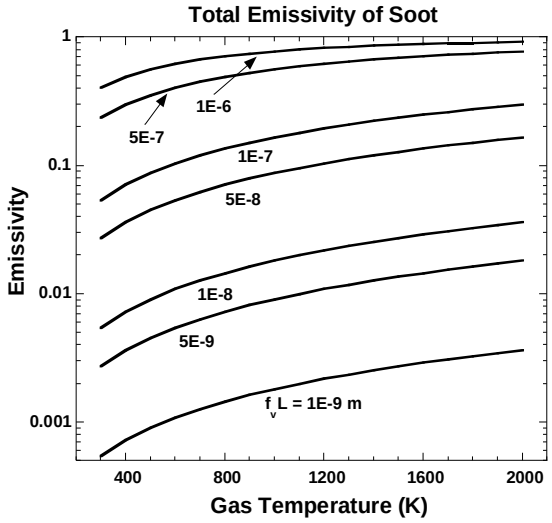

Fig. 6a. Calculated total emissivity of soot particulates using OpenSC.

In practical engineering calculations, H_2O, CO_2, and/or soot particulates can simultaneously exist in a mixture. The total emissivity behavior associated with such mixture along a line of sight is limited in currently available literature except for those found in [13]. In order to provide a more comprehensive overview of mixture emissivity behavior to the reader, examples are generated by OpenSC to demonstrate the effect of different combination of gaseous species and soot particulates.

Fill in Input Values: Total Pressure = 1 atm (101 kPa)

Mixture Properties	Single Value Calculation		Range Calculation			
	Select	Value	Select	Minimum Value	Maximum Value	Number of Steps (>=2)
Soot Volume Fraction Pathlength (m): 0 to 0.000001	◉	0.000000001	○			
Temperature (K): 300 to 2000	○		◉	300	2000	18
$CO_2/(CO_2+H_2O)$ Mole Fraction: 0.0 to 1.0	◉	0	○			
Pressure Pathlength (kPa-m): 0 to 2000 (< Path Length x 1 atm)	◉	0	○			
Path Length (m): > 0	◉	1	○			
Source Temperature (K): 300 to 1500	◉	300	○			

Calculate

Download Results to File

Fig. 6b. Inputs for the evaluation of pure soot emissivity at different gas temperature (since the soot concentration is not evenly distributed, manual input is needed to handle calculations for 7 different soot concentrations).

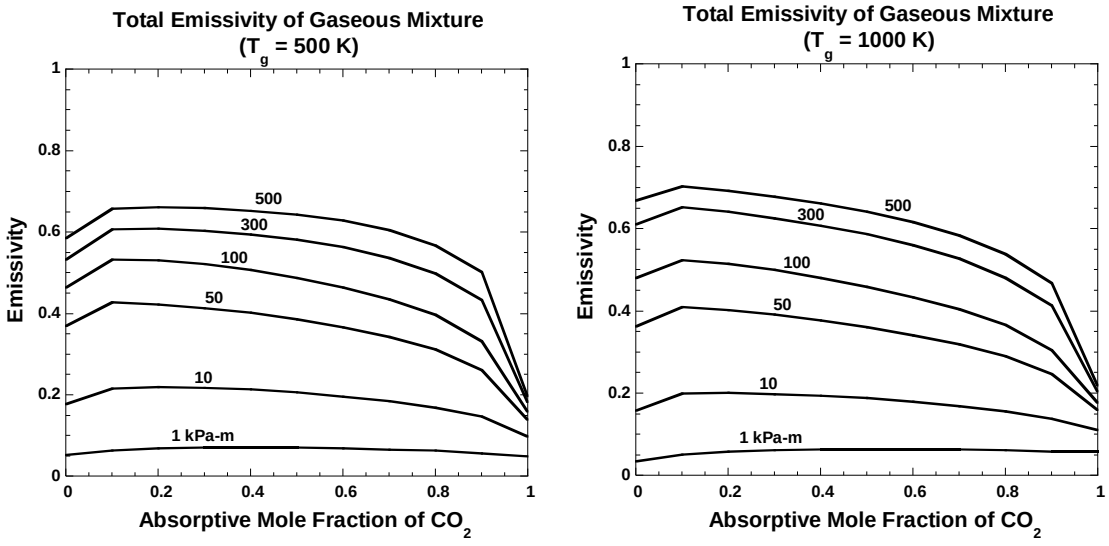

Figs 7a. Calculated total emissivity of mixture consisted of water vapor and carbon dioxide with gas temperature evaluated at 500 K (left) and 1000 K (right) using OpenSC.

In Figs. 7a, the total emissivity of a mixture of H_2O and CO_2 is plotted as a function of the absorptive mole fraction of CO_2 with different absorptive optical thicknesses. A typical input file for the generation of the numerical data is shown in Fig. 7b. Two gas temperatures, 500 K and 1000 K, are considered in this example. In general, the mixture emissivity increases with increasing absorptive optical thickness and this emissivity behavior is independent of gas temperature. For different fractions of CO_2, it is interesting to see that CO_2 addition to the mixture first increases and then decreases the mixture emissivity. The initial increases of the mixture emissivity in the region of low CO_2 fraction is primarily due to the strong absorption effect from the fundamental band CO_2 (4.3 μm) and the overlapping effect associated with the

absortion band of H_2O (2.7 μm) and CO_2 (2.7 μm) near the peak of Planck function for 1000 K (2.9 μm)[4]. A "small" amount of CO_2 added to the mixture thus increase the mixture emissivity. However, as the CO_2 concentration increases, the H_2O contribution to the mixture emissivity decreases and the mixture emissivity decreases toward the total emissivity of pure CO_2 (refer to Fig. 5a). Fig. 8 shows the emissivity of mixture consisted of H_2O, CO_2, and soot particulates and, as expected, the mixture emissivity generally increases with increasing soot concentration.

Fill in Input Values: Total Pressure = 1 atm (101 kPa)

Mixture Properties	Single Value Calculation		Range Calculation			
	Select	Value	Select	Minimum Value	Maximum Value	Number of Steps (>=2)
Soot Volume Fraction Pathlength (m): 0 to 0.000001	◉	0	○			
Temperature (K): 300 to 2000	○		◉	500	1000	2
$CO_2/(CO_2+H_2O)$ Mole Fraction: 0.0 to 1.0	◉	1	○			
Pressure Pathlength (kPa-m): 0 to 2000 (< Path Length x 1 atm)	○		◉	0	1	11
Path Length (m): > 0	◉	1	○			
Source Temperature (K): 300 to 1500	◉	300	○			

Calculate

Download Results to File

Fig. 7b. Inputs for the evaluation of mixture emissivity with different absorptive mole fraction of CO_2 as a function of gas temperature.

3.1.2 Absorptivity

Total absorptivity is an important parameter that characterizes the total amount of energy being absorbed by a medium due to emission from another source. Fundamentally, the total absorptivity from non-gray gases can have a completely different behavior as compared to the total emissivity if the source temperature differs from the gas temperature. However, if the mixture is assumed to be gray, the total absorptivity is constrained to be equal to the total emissivity, an assumption generally invoked without any mathematical verification in many fire applications (for example, this practice is found in one of the most commonly used fire simulation codes[5] [25] certified by the U.S. Department of Energy). Since the effect of radiation is known to be not only important, but dominant in combustion/fire calculations. OpenSC can be used to obtain the total absorptivity of a mixture consisting of H_2O, CO_2, and/or soot particulates for different conditions and the obtained results can be used to assess the accuracy of the gray assumption of equal total absorptivity and total emissivity.

[4] The peak of Planck function is determined from solving the Wien's displacement law with a gas temperature.

[5] The fire simulation code is typically being used to predict the environment in a multi-compartment structure subjected to a fire and/or to simulate the impact of past or potential fires and smoke in a specific building environment by fire investigators, safety officials, engineers, architects, and builders.

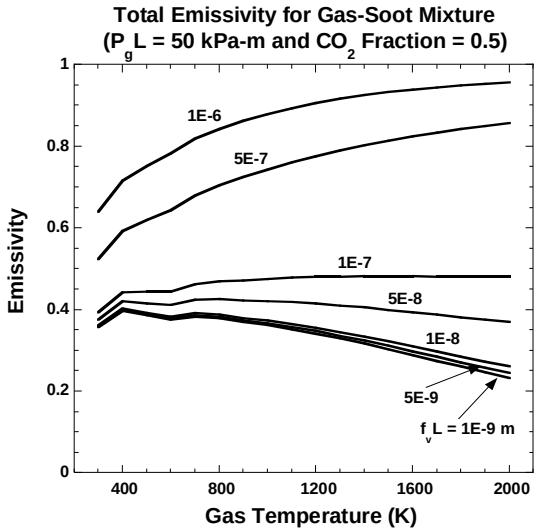

Fig. 8. Calculated total emissivity of soot-gas mixture using OpenSC.

Fill in Input Values: Total Pressure = 1 atm (101 kPa)

Mixture Properties	Single Value Calculation		Range Calculation			
	Select	Value	Select	Minimum Value	Maximum Value	Number of Steps (>=2)
Soot Volume Fraction Pathlength (m): 0 to 0.000001	○		◉	0	0.0000001	2
Temperature (K): 300 to 2000	○		◉	300	2000	18
$CO_2/(CO_2+H_2O)$ Mole Fraction: 0.0 to 1.0	◉	10	○			
Pressure Pathlength (kPa-m): 0 to 2000 (< Path Length x 1 atm)	◉	0.5	○			
Path Length (m): > 0	◉	1	○			
Source Temperature (K): 300 to 1500	○		◉	500	1500	3

Calculate

Download Results to File

Fig. 9. Inputs for the evaluation of mixture emissivity and absorptivity as a function of gas temperature with 3 different source temperatures for 2 soot conditions.

3.1.3 Comparison between absorptivity and emissivity

Fig. 9 shows a typical input file for the determination of absorptivity and emissivity of mixture consisted of H_2O, CO_2, and/or soot particulates. In contrast to the evaluation of total emissivity, the source temperature is now important. For a gas mixture, the total emissivity and the total absorptivity as a function of gas temperature are plotted in Fig. 10. Three different source temperatures (500 K, 1000 K, and 1500 K) for the total absorptivity are considered in the example. Since the total emissivity is independent of source temperature, there is only one curve for the total emissivity. As shown in the figure, the total absorptivity is significantly different than the total emissivity both in terms of its numerical value and its dependence on the gas temperature. In general, the total absorptivity is an increasing function of gas temperature, which is completely opposite to the trend for the total emissivity. For the effect of source temperature, it can be noticed that lower source temperature typically leads to

overall higher total absorptivity. Physically, this trend is expected because the peak of the Planck function for lower source temperature is shifted to the more active absorption band for H_2O in the long wavelength region (4.7 μm and 6.3 μm). The total absorptivity for a soot-gas mixture is presented in Fig. 11. Note that the gas temperature has an effect on the total absorptivity only for a gas-soot mixture with a finite absorptive optical thickness (P_gL = 10 kPa-m in Fig. 11). In the limit of a pure soot mixture, the total absorptivity is only a function of the source temperature.

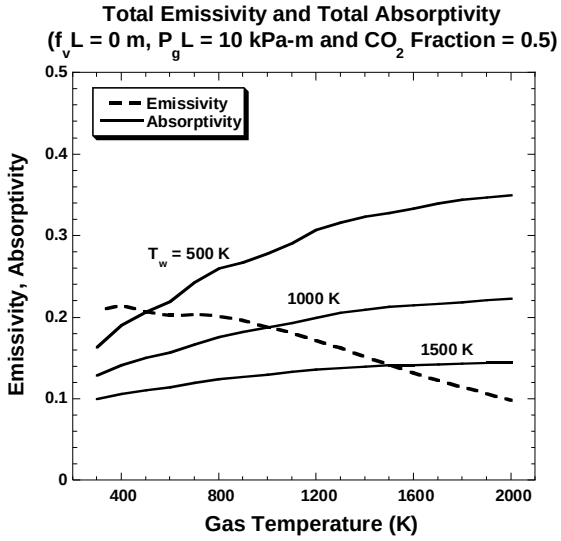

Fig. 10. Absorptivity of gas mixture (no soot) at different source temperature (Emissivity of the same mixture is also plotted for comparison).

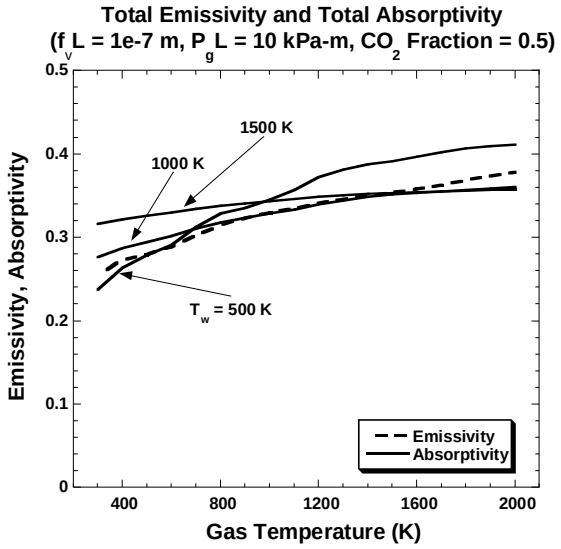

Fig. 11. Absorptivity of soot-gas mixture at different source temperature (Emissivity of the same mixture is also plotted for comparison).

Quantitatively, comparison between the total emissivity and the total absorptivity as shown in Fig. 10 and 11 demonstrates clearly that the two properties are different and have different dependence on mixture parameters. Therefore, the assumption of a gray medium with equal emissivity and absorptivity

for the combustion products is not supported by fundamental physics and should not be applied for the evaluation of radiation effect for non-gray medium in fire design/safety protection calculations.

3.2 Assessment of the Emissivity Chart Model

Accurate evaluation of radiative properties for combustion mixtures with H_2O, CO_2, and soot particulates is difficult for engineers/non-radiation experts because they generally do not have the required skills or computational resources to carry out such a complex and detailed radiation calculation. In the fire safety community, it is a common practice that the effect of radiation is evaluated based on approximations/simplified methods suggested in engineering handbooks [14,15]. However, many of these approximations and/or simplified methods documented in existing engineering handbooks have not been rigorously validated. Therefore, their accuracy can be highly uncertain. In this section, results generated from OpenSC will be used to assess the predictions obtained from these approximations or simplified methods provided in handbooks [14,15]. Specifically, the accuracy of the emissivity chart model will be examined.

3.2.1 Emissivity

In the most recently published SFPE Fire Protection Engineering Handbook [14], the total emissivity for a homogeneous mixture consisted of H_2O and CO_2 is determined based on the graphical interpolation from total emissivity charts. In general, the total emissivity charts refer to those appearing in Edwards [15] which are the modified emissivity charts first introduced by Hottel and his co-workers [6] based on their experimental measurements. Specifically, these charts are expressed in correlations with gas temperature and absorptive partial pressure pathlength as the input parameters:

$$\varepsilon_g = \varepsilon\left(p_a L, p, T_g\right) \tag{14}$$

where p_a is the partial pressure of the gaseous species, p is the total gas pressure, and T_g is the gas temperature. Emissivity charts are only available for a pure CO_2/N_2 and a pure H_2O/N_2 mixture. For gas mixture consisted of both H_2O and CO_2, the total emissivity is determined from the following expression

$$\varepsilon_g = C_{H_2O}\,\varepsilon_{H_2O} + C_{CO_2}\varepsilon_{CO_2} - \Delta\varepsilon \tag{15}$$

with C_{H_2O}, C_{CO_2}, and $\Delta\varepsilon$ being the correction factor for H_2O, the correction factor for CO_2, and the band overlap correction, respectively. Following the calculation guidelines provided in [14], it is assumed that the pressure correction factors are 1.0 and the band overlap correction is approximated to be $\Delta\varepsilon = 1/2\ \varepsilon_{CO_2}$. With these approximations, the total emissivity is simplified to be

$$\varepsilon_g \approx \varepsilon_{H_2O} + \frac{1}{2}\,\varepsilon_{CO_2} \tag{16}$$

where the effect of the emission from a H_2O and CO_2 mixture is approximated to be the sum of the effect of full emission from H_2O and the reduced emission effect from CO_2. For soot-gas mixture, the total emissivity is given by

$$\varepsilon_t = (1 - e^{-\kappa_s L}) + \varepsilon_g e^{-\kappa_s L} \tag{17}$$

with κ_s being the effective absorption coefficient of the soot. In Eq. (17), the total emissivity of the soot-gas mixture is approximated to be a linear summation of the soot emission and the gas emission being transmitted through the soot. The effective soot absorption coefficient, κ_s, is generated by an exponential curve-fit of the emissivity data for a pure soot mixture [25]. For typical fuels, κ_s is taken to be kf_vT_g with the optical constant k suggested to be 1800. Based on Eq. (17), ones can determine the pure soot emissivity to be

$$\varepsilon_s = 1 - e^{-kf_vT_gL} \tag{18}$$

Fig. 12a and 12b present the total emissivity for pure H_2O/N_2 and pure CO_2/N_2 mixtures as a function of gas temperature for a wide range of optical thickness generated by OpenSC and the emissivity chart model, respectively. The benchmark emissivity obtained from the LBL method [26,27], as shown in dashed lines, is provided for reference. From the two figures, it can be readily observed that the OpenSC prediction of the pure H_2O/N_2 and CO_2/N_2 emissivity is comparable to that of the total emissivity chart and both predictions have the same relative accuracy as compared to the LBL prediction. For both the H_2O/N_2 and CO_2/N_2 mixtures, the largest discrepancy among the three models occurs in the region of large optical thickness. For the OpenSC prediction, the discrepancy with the "exact" LBL model can be attributed to both the assumption of the narrow-band model [26-28], as well as the experimental error associated with the data used to generate RADCAL. For the emissivity chart prediction, the discrepancy with the "exact" LBL model is entirely due to experimental uncertainty, particularly in the acquisition of emissivity data in mixtures with high absorptive gas concentration. From the perspective of practical application in combustion scenarios in which relative significant uncertainty may exist in the measurement of many combustion parameters (temperature and partial pressure of absorptive gases), both the OpenSC and the emissivity charts are acceptable to be used to estimate the effect of radiation heat transfer for pure H_2O/N_2 and pure CO_2/N_2 mixture.

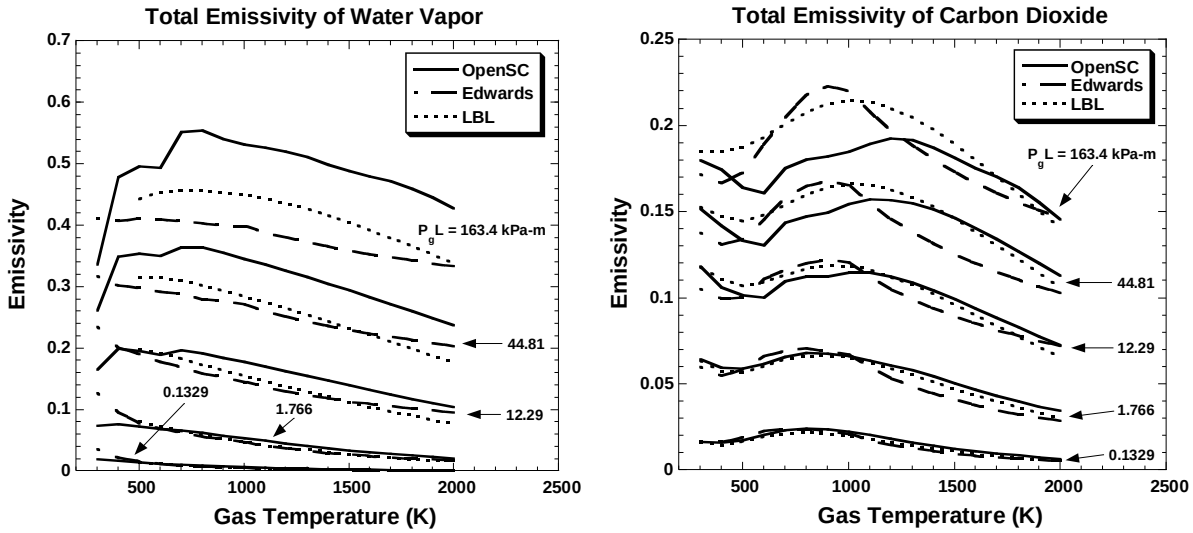

Figs. 12. Approximate total gas emissivity for a) H_2O and b) CO_2 together with the results generated by OpenSC, the emissivity charts of Edwards, and LBL method.

Figs. 13 show the total emissivity for gas mixture consisted of H_2O and CO_2 predicted by OpenSC and the emissivity chart. It is important to note that there is no "exact" solution for mixture emissivity as

the LBL approach for mixtures is numerically complex. For the emissivity chart model, the overlapping effect for H_2O and CO_2 is simulated using the approximation given in Eq. (16). For OpenSC, the narrow-band absorption coefficient of the species generated by RADCAL (which accounts for the overlapping effect of the species with the narrow-band model) is used to evaluate the spectral transmissivity and the total emissivity is obtained by direct integration over all wavelengths. The evaluation of mixture emissivity by OpenSC is thus expected to have the same level of accuracy as that for a pure gas and can serve as an approximate benchmark to compare to the emissivity chart model. Results in Fig. 13a and 13b show that while OpenSC and the emissivity chart model yield the same qualitative effect of mixture ratio, optical thickness and temperature for the mixture emissivity, Eq. (16) generally under-predicts the mixture emissivity for nearly the entire range of the different parameters. Therefore, the suitability of the ad-hoc approach for the emissivity chart model to properly account for the effect of mixture, as represented in Eq. (16), is brought into question for practical engineering applications.

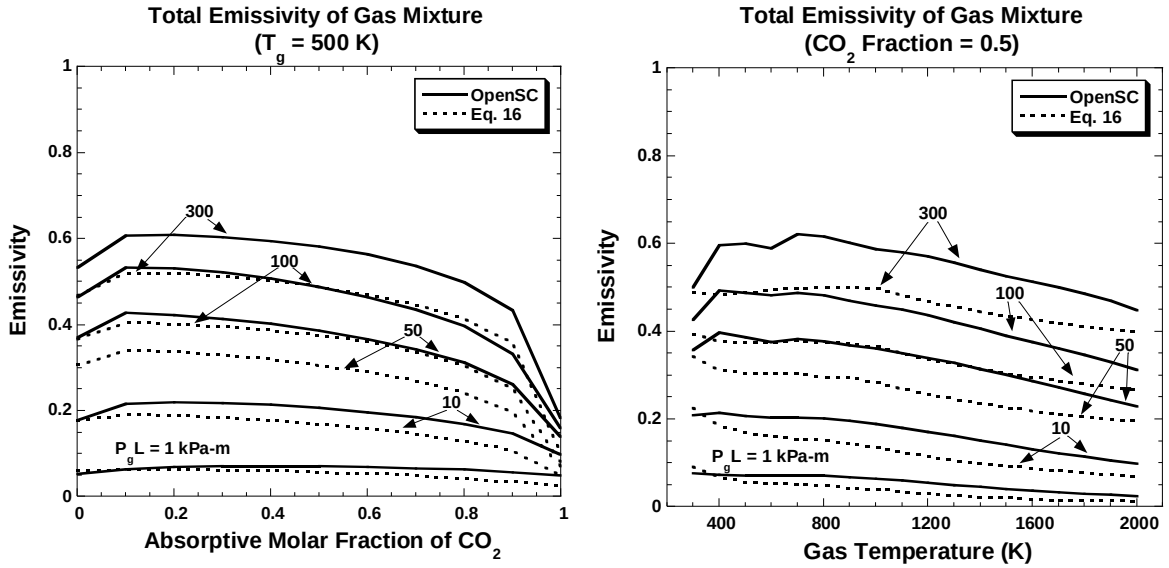

Figs. 13. Total mixture emissivity with a range of optical thickness a) as a function of CO_2 fraction for gas temperature at 500 K (left) and b) as a function for gas temperature for CO_2 fraction of 0.5 (right).

Total emissivity of soot particulates obtained based on Eq. (18) and that of generated from OpenSC are shown in Fig. 14. As expected, soot emissivity from both sets of data is increasing function of increasing temperature. Since the soot absorption coefficient used in Eq. (18) is obtained by a "best fit" of the analytical solutions (Eq. 5) used by OpenSC [24], the two models are in reasonable agreement and both can be used for practical engineering applications.

Figs. 15 show the total emissivity for the soot-gas mixture. In Fig. 15a, the mixture emissivity is plotted as a function of gas temperature with various optical thicknesses for a CO_2 fraction of 0.5 and a soot concentration thickness of 10^{-7} m. Compared to the pure mixture results presented in Fig. 13b, the addition of soot enlarges the discrepancy between OpenSC and the emissivity chart model. Physically, the inverse temperature behavior of the soot absorption coefficient is not captured by Eq. (17) and this leads to an increase in the error for the prediction from using the emissivity chart model at high temperature. Fig. 15b shows the mixture emissivity as a function of gas temperature with various soot concentration for a particular optical thickness and a CO_2 fraction. In general, the discrepancy between OpenSC and the emissivity chart model is significant.

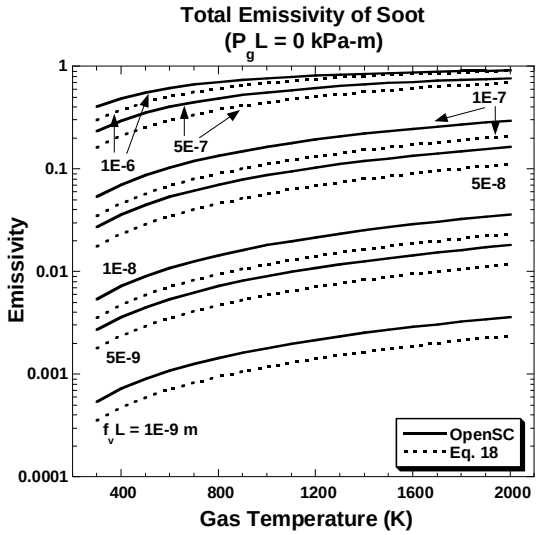

Fig. 14. Total emissivity for soot particulates in logarithmic scale.

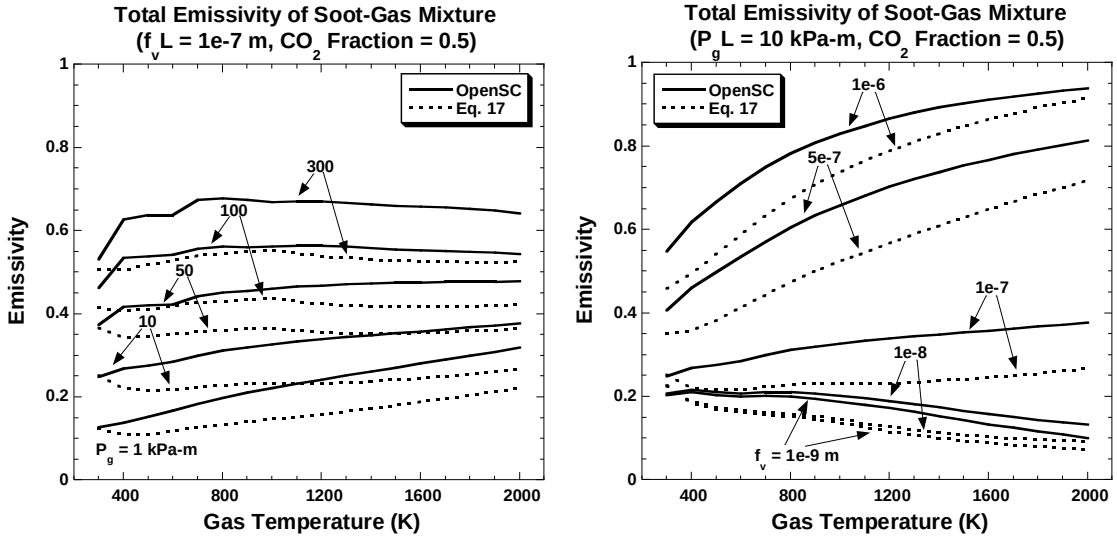

Figs. 15. Total soot-gas mixture emissivity a) with a range of optical thickness as a function of gas temperature for soot concentration of 1e-7 m and CO_2 fraction of 0.5 (left) and b) with a range of soot concentration as a function of gas temperature for optical thickness of 10 kPa-m and CO_2 fraction of 0.5 (right).

3.2.2 Absorptivity

For calculation convenience and/or computation efficiency, the empirical ad-hoc approach used by the emissivity chart model for the evaluation of the total absorptivity of a homogeneous gas mixture is to modify the spectrally integrated emissivity to become absorptivity using the Hottel's or Penner's Rule [15]. Specifically, the rule is to first evaluate the gas emissivity at the source temperature T_w and then multiply the emissivity by a factor of $(T_g/T_w)^{1/2}$ to generate the value of the total absorptivity. Mathematically, the total absorptivity is approximated to be

$$\alpha_g = \alpha\left(p_a L, p, T_g, T_w\right) = \varepsilon_g(p_a L, p, T_w)\left(\frac{T_g}{T_w}\right)^{\frac{1}{2}} \tag{19}$$

In OpenSC, the evaluation of the total absorptivity differs from that of the total emissivity only in the specification of the source temperature. Since the numerical integration requires no additional assumptions, the OpenSC prediction for the absorptivity is expected to have the same degree of accuracy as that for the total emissivity. OpenSC can thus serve as an approximate benchmark solution to assess the accuracy of Eq. (19).

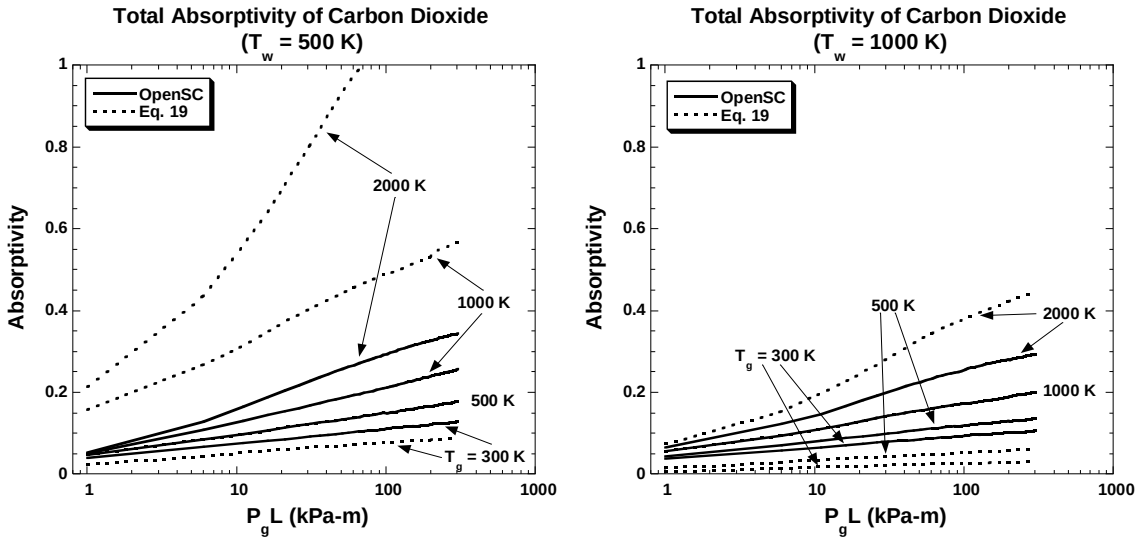

Figs. 16. Total absorptivity of CO_2 for a) T_w = 500 K (left) and b) T_w = 1000 K (right) together with the results generated from OpenSC.

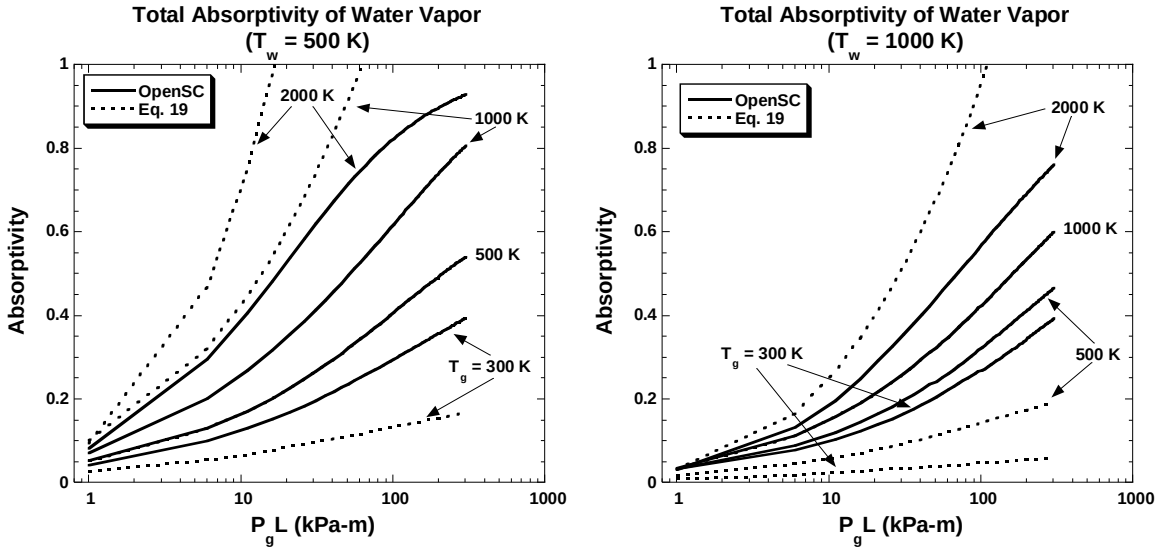

Figs. 17 Total absorptivity of H_2O for a) T_w = 500 K (left) and b) T_w = 1000 K (right) together with the results generated from OpenSC.

Comparison between results generated from OpenSC and the approximate absorptivity generated by Eq. (19) at different source temperature T_w for pure CO_2/N_2 and pure H_2O/N_2 mixture is shown in Figs. 16 and 17, respectively. It is apparent that while Eq. (19) yields the correct qualitative behavior that the absorptivity increases with increasing gas temperature T_g, the approximation should not be relied upon in engineering calculations when the source and gas temperatures differ by more than a small amount. For

reference, Fig. 18 show the total absorptivity obtained from OpenSC and that of generated from Eq. (19) together with the total emissivity for a typical combustion condition. It can be seen that similar discrepancy appears for both radiative properties as a function of gas temperature.

In summary, OpenSC and the general emissivity chart have the same order of accuracy in predicting the total emissivity of a mixture consisting only one absorptive gas species (H_2O or CO_2). OpenSC is expected to have the same order of accuracy for gas mixtures with multiple species and also the absorptivity of a gas mixture. Using the OpenSC results as benchmark, the emissivity chart model and its ad-hoc modifications for mixture and absorptivity are shown to be in significant error. To highlight the error of the emissivity chart model associated with the example calculations presented in Figs. 13 to 17 quantitatively, the percentage error of the emissivity chart prediction, Er, is evaluated as follow

$$Er = \frac{\left(X_{OpenSC} - X_{emissivity\ chart}\right)}{X_{OpenSC}} \text{ x } 100 \tag{20}$$

where X_{OpenSC} is the OpenSC prediction and $X_{emissivity\ chart}$ is the prediction obtained from the emissivity chart model. For the total emissivity shown in Figs. 13, 14, and 15, the average Er is approximately 23.3 %, 28.2 %, and 22.7 %, respectively. For total absorptivity shown in Figs. 16 and 17, the average value of Er is approximately 137.7 % and 64.1 %, respectively.

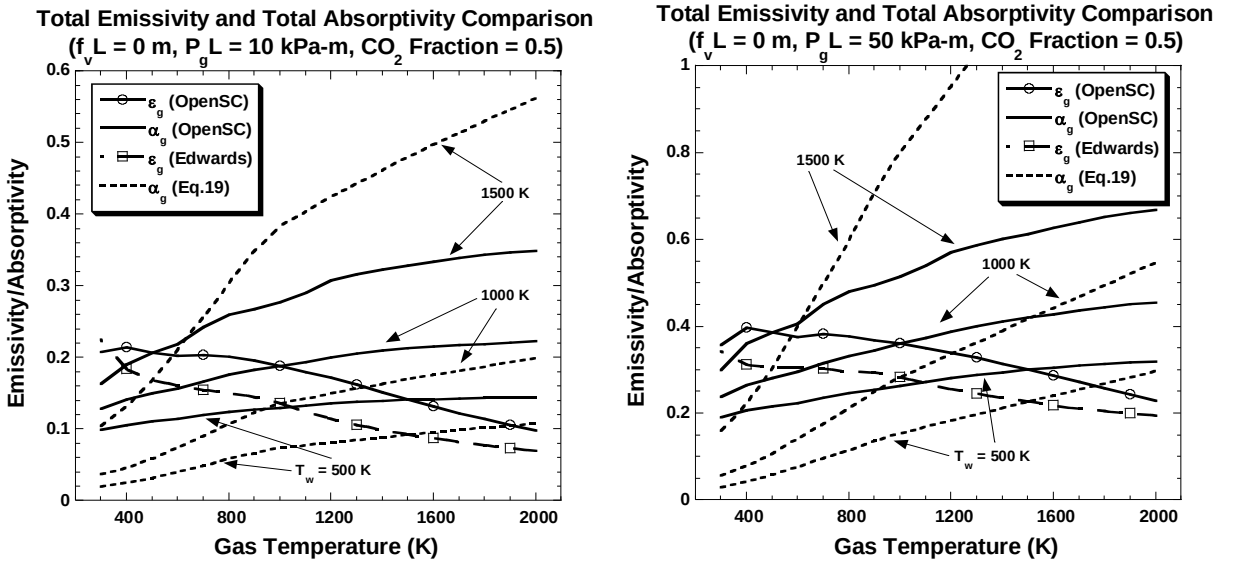

Figs. 18. Total absorptivity of soot-gas mixture as a function of gas temperature with 3 different source temperatures for a) P_gL = 10 kPa-m (left) and b) P_gL = 50 kPa-m (right) with emissivity of the same mixture plotted for comparison).

4. CONCLUSIONS

OpenSC, an Open-source Spectral Calculation Tool, for the determination of radiative properties of a homogenous combustion mixture consisted of H_2O, CO_2, and/or soot particulates, is presented. The mathematical formulation and the neural network correlations used in OpenSC are described.

Numerical examples of total emissivity/absorptivity for various mixture conditions are presented to illustrate the capability of the calculation tool. Based on direct comparison with the benchmark results from the LBL method, OpenSC and the total emissivity charts recommended in the SFPE Fire Protection Handbooks are shown, generally, to have the same degree of accuracy for the prediction of emissivity for pure H_2O/N_2 and pure CO_2/N_2 mixture.

For mixtures consisted of H_2O, CO_2, and/or soot particulates, OpenSC is used as the benchmark to assess the gray assumption of radiative properties. Quantitative comparisons show that the total emissivity is generally different from the total absorptivity and they have completely different dependence on mixture conditions. Therefore, the gray assumption of equal total emissivity and total absorptivity is generally not valid.

The emissivity chart approach suggested by the SFPE Fire Protection Handbooks for the evaluation of mixture emissivity and mixture absorptivity are assessed. In comparison to the results generated from OpenSC, the emissivity chart approach generally under-predicts the mixture emissivity. For mixture absorptivity, the discrepancy in between OpenSC and the emissivity approaches is substantial.

5. ACKNOWLEDGEMENTS

The authors would first like to acknowledge the brilliant insight of Dr. William Grosshandler in developing the RADCAL model which provides the foundation for the development of OpenSC. We would also like to thank Dr. Grace Ngai from the Computing Department at the Hong Kong Polytechnic University for her guidance on the initial implementation of PHP in the development of OpenSC and Dr. Jiann C. Yang from NIST for his constructive comments and valuable suggestions to this manuscript.

6. HYPERLINK AND SOURCE CODE FOR OPENSC

OpenSC can be accessed in the following hyperlink: http://walter-yuen.com/RADNNET/

Source code can be obtained from https://github.com/wnt2/OpenSC

7. REFERENCES

1. Modest, M. F. (2013). The treatment of nongray properties in radiative heat transfer: from past to present. *Journal of Heat Transfer*, 135(6), 061801.

2. Wang, L., Modest, M. F., Haworth, D. C., and Turns, S. R., 2005, "Modeling Non-gray Soot and Gas-Phase Radiation in Luminous Turbulent Non premixed Jet Flames," *Combust. Theory Model.*, 9(3), pp. 479–498.

3. Modest, M. F., 2013, *Radiative Heat Transfer*, 3rd ed., Academic, New York.

4. Rothman, L. S., Gordon, I. E., Barber, R. J., Dothe, H., Gamache, R. R., Goldman, A., Perevalov, V. I., Tashkun, S. A., and Tennyson, J., 2010, "HITEMP, the High- Temperature Molecular Spectroscopic Database," *J. Quant. Spectrosc. Radiat. Transfer*, 111(15), pp. 2139–2150.

5. Grosshandler, W. L., 1993, "RADCAL: A Narrow-Band Model for Radiation Calculations in a Combustion Environment," *NIST Technical Note* 1402, National Institute of Standards and Technology.

6. Hottel, H. C., 1954, "Radiant Heat Transmission," *Heat Transmission*, 3rd ed., W. H. McAdams, ed., McGraw-Hill, New York, Chap. 4.

7. Hottel, H. C., and Sarofim, A. F., 1967, *Radiative Transfer*, McGraw-Hill, New York.

8. McGrattan, K., Hostikka, S., Floyd, J., Baum, H., Rehm, R. G., Mell, W., & McDermott, R. (2010). Fire dynamics simulator (version 5), technical reference guide. *NIST special publication*, 1018(5).

9. Edwards, D. K., 1976, "Molecular Gas Band Radiation," *Advances in Heat Transfer*, Vol. 12, Academic, New York, pp. 115–193.

10. Tam, W.C. and Yuen, W. W., 2018, "Assessment of Radiation Solvers for Fire Simulation Models Using RADNNET-ZM," 11th AOSFST, Taiwan.

11. Yuen, W. W., Chow, C. L., & Tam, W. C. (2016). Analysis of radiative heat transfer in inhomogeneous nonisothermal media using neural networks. *Journal of Thermophysics and Heat Transfer*, *30*(4), 897-911.

12. Yuen, W. W., Tam, W. C., & Chow, W. K. (2014). Assessment of radiative heat transfer characteristics of a combustion mixture in a three-dimensional enclosure using RAD-NETT (with application to a fire resistance test furnace). *International Journal of Heat and Mass Transfer*, *68*, 383-390.

13. Yuen, W. W. (2009). RAD-NNET, a neural network-based correlation developed for a realistic simulation of the non-gray radiative heat transfer effect in three-dimensional gas-particle mixtures. *International Journal of Heat and Mass Transfer*, *52*(13-14), 3159-3168.

14. Hurley, M. J., Gottuk, D. T., Hall Jr, J. R., Harada, K., Kuligowski, E. D., Puchovsky, M., ... & Wieczorek, C. J. (Eds.). (2016). *SFPE handbook of fire protection engineering*. Springer.

15. Edwards, D. K. (1985). in *Handbook of Heat Transfer Fundamentals*, McGraw-Hill, New York.

16. Lallemant, N., & Weber, R. (1996). A computationally efficient procedure for calculating gas radiative properties using the exponential wide band model. *International Journal of Heat and Mass Transfer*, *39*(15), 3273-3286.

17. ESoufiani, A., and Taine, J., 1997, "High Temperature Gas Radiative Property Parameters of Statistical Narrow-Band Model for H_2O, CO_2, and CO, and Correlated- k Model for H_2O and CO_2," *Int. J. Heat Mass Transfer*, 40(4), pp. 987–991.5.

18. Smith, T. F., Shen, Z. F., and Friedman, J. N., 1982, "Evaluation of Coefficients for the Weighted Sum of Gray Gases Model," ASME J. Heat Transfer, 104(4), pp. 602–608.

19. Bohren, C. F., & Huffman, D. R. (2008). *Absorption and scattering of light by small particles*. John Wiley & Sons.

20. Howell, J. R., Menguc, M. P., & Siegel, R. (2015). *Thermal radiation heat transfer*. CRC press.

21. Selamet, A., & Arpaci, V. S. (1989). Rayleigh limit—Penndorf extension. *International Journal of Heat and Mass Transfer*, *32*(10), 1809-1820.

22. Dalzell, W. H., & Sarofim, A. F. (1969). Optical constants of soot and their application to heat-flux calculations. *Journal of Heat Transfer*, *91*(1), 100-104.

23. Lecoustre, V. R., Wakatsuki, K., & Jackson, G. S. (2014). Fitting narrow-band models to temperature-dependent, spectral absorption coefficients of fuel vapors. *Journal of Quantitative Spectroscopy and Radiative Transfer*, *147*, 24-37.

24. Yuen, W. W., & Tien, C. L. (1977, January). A simple calculation scheme for the luminous-flame emissivity. In *Symposium (International) on Combustion* (Vol. 16, No. 1, pp. 1481-1487). Elsevier.

25. Peacock, R. D., Jones, W., Reneke, P., & Forney, G. (2005). CFAST–Consolidated Model of Fire Growth and Smoke Transport (Version 6) User's Guide. *NIST Special Publication*, *1041*.

26. Alberti, M., Weber, R., & Mancini, M. (2015). Re-creating Hottel's emissivity charts for carbon dioxide and extending them to 40bar pressure using HITEMP-2010 data base. *Combustion and Flame*, *162*(3), 597-612.

27. Alberti, M., Weber, R., & Mancini, M. (2016). Re-creating Hottel's emissivity charts for water vapor and extending them to 40 bar pressure using HITEMP-2010 data base. *Combustion and Flame*, *169*, 141-153.

28. Alberti, M., Weber, R., Mancini, M., & Modest, M. F. (2013). Comparison of models for predicting band emissivity of carbon dioxide and water vapour at high temperatures. *International Journal of Heat and Mass Transfer*, *64*, 910-925.

8. APPENDICES

Appendix A: Tabulated Values for Pentagamma Function

For ease of reference, Eq. (6) is rewritten as

$$\alpha_s(T_w, f_v L) = 1 - \frac{15}{\pi^4} y(x)$$

with

$$y(x) = \psi^{(3)}(x) \ , \qquad \text{for } x = 1 + \frac{cT_w L}{C_2}$$

and the tables in below provide the tabulated values of the pentagamma function of x for the determination of soot absorptivity.

x	y(x)
1	6.49393
1.01	6.25106
1.02	6.01969
1.03	5.79918
1.04	5.58892
1.05	5.38832
1.06	5.19687
1.07	5.01404
1.08	4.8394
1.09	4.67248
1.1	4.51288
1.11	4.36021
1.12	4.21411
1.13	4.07424
1.14	3.94029
1.15	3.81194
1.16	3.68892
1.17	3.57096
1.18	3.4578
1.19	3.34922
1.2	3.24499
1.21	3.14491
1.22	3.04876
1.23	2.95637
1.24	2.86755
1.25	2.78214

x	y(x)
1.26	2.69999
1.27	2.62094
1.28	2.54485
1.29	2.47159
1.3	2.40102
1.31	2.33304
1.32	2.26752
1.33	2.20436
1.34	2.14346
1.35	2.08471
1.36	2.02803
1.37	1.97332
1.38	1.92051
1.39	1.86952
1.4	1.82026
1.41	1.77268
1.42	1.72668
1.43	1.68222
1.44	1.63923
1.45	1.59766
1.46	1.55744
1.47	1.51852
1.48	1.48086
1.49	1.4444
1.5	1.40909
1.51	1.3749

x	y(x)
1.52	1.34177
1.53	1.30968
1.54	1.27857
1.55	1.24842
1.56	1.21918
1.57	1.19082
1.58	1.16332
1.59	1.13664
1.6	1.11074
1.61	1.08561
1.62	1.06122
1.63	1.03753
1.64	1.01452
1.65	0.992176
1.66	0.970466
1.67	0.949371
1.68	0.928868
1.69	0.908938
1.7	0.889562
1.71	0.87072
1.72	0.852395
1.73	0.834569
1.74	0.817226
1.75	0.80035
1.76	0.783925
1.77	0.767937

x	y(x)
1.78	0.752371
1.79	0.737215
1.8	0.722455
1.81	0.708077
1.82	0.694071
1.83	0.680425
1.84	0.667126
1.85	0.654165
1.86	0.641531
1.87	0.629213
1.88	0.617203
1.89	0.60549
1.9	0.594067
1.91	0.582923
1.92	0.572051
1.93	0.561442
1.94	0.55109
1.95	0.540985
1.96	0.531121
1.97	0.521492
1.98	0.512089
1.99	0.502907
2	0.493939

Appendix B: Neural Network Elements associated with a Mixture Condition

With the following neural network elements provided in below tables, the neural network correlation as shown in Eq. 12 – 14 can be used to determine the total absorptivity for the following ranges of input parameters 1) $300\ \text{K} \leq T_w, T_g \leq 2000\ \text{K}$, 2) $10 \leq P_g L \leq 50$ kPa-m, 3) $0 \leq X_{CO_2} \leq 1.0$, and 4) $0 \leq f_v L \leq 10^{-6}$ m. It should be noted that the floating-point format of the original set of neural network elements is in double precision.

W_{ij}^1	j = 1	j = 2	j = 3	j = 4	j = 5
i = 1	1.25E+00	-7.04E-01	3.99E-02	2.70E-01	1.02E-02
i = 2	1.81E-01	4.66E-01	1.83E-01	-7.31E-02	-2.68E-03
i = 3	-2.15E-02	-2.67E+00	5.29E-01	-1.25E-01	1.65E-02
i = 4	2.16E-02	-5.42E+00	6.73E-02	-1.13E-02	-9.90E-03
i = 5	-2.53E-01	-1.07E-01	-1.11E+01	6.59E-02	4.94E-03
i = 6	-3.44E-01	5.38E-01	-4.89E-01	1.96E-01	2.04E-03
i = 7	9.81E-02	-2.39E+00	-7.40E-02	1.59E-01	-2.88E-03
i = 8	-2.34E-02	8.88E-01	7.58E-01	-2.34E-01	-1.31E-03
i = 9	-2.45E+00	-2.13E-02	-2.02E-01	-9.59E-02	-5.35E-03
i = 10	2.07E-01	9.06E-01	1.32E-01	-1.74E-01	-1.16E-03
i = 11	-1.09E+00	3.16E-01	-8.36E-01	-3.37E-01	4.70E-02
i = 12	-1.28E+00	8.49E-02	1.40E+00	1.16E-01	-4.80E-02
i = 13	3.06E-01	-1.81E-02	1.79E-01	-6.23E-02	1.56E-03
i = 14	2.66E-01	-1.67E-01	-2.41E-01	3.22E-01	1.09E+00
i = 15	1.95E-01	1.13E-01	-3.16E+00	-1.39E-01	7.53E-03
i = 16	1.16E-01	1.70E-01	1.18E-01	-6.84E-02	1.60E+00
i = 17	-1.81E-01	-1.28E-01	1.67E-01	-1.16E+00	3.67E-02
i = 18	-3.14E-01	1.39E-01	-2.57E-01	-6.27E-01	4.94E-04

Table B1: Values of the weight matrix W_{ij}^1 for exceed absorptivity at $P_g L$ ranging from 10 kPa-m to 50 kPa-m.

W_{ij}^2	j = 1	j = 2	j = 3	j = 4	j = 5	j = 6	j = 7	j = 8
i = 1	-2.47E-01	-1.07E-01	-5.00E-01	-9.88E-01	-8.15E-01	-9.87E-01	5.96E-01	1.19E+00
i = 2	-5.71E-01	7.34E-03	-3.64E-01	9.20E-02	-5.86E-03	-4.76E-01	1.02E+00	-5.25E-02
i = 3	-4.29E-01	6.78E-01	1.79E-01	-1.40E-01	-8.92E-01	8.35E-01	3.75E-01	6.65E-01
i = 4	-4.36E-01	-1.02E-02	-5.16E-02	-2.90E-01	-2.34E-01	4.82E-01	-3.97E-01	-9.59E-01
i = 5	4.43E-03	-1.70E+00	-2.90E-01	-1.19E-01	2.41E-01	-4.70E-01	-1.79E-01	9.58E-02
i = 6	-2.52E-02	-4.20E-01	-7.06E-02	-6.64E-02	-2.14E+00	7.91E-03	8.62E-03	7.60E-02
i = 7	-4.37E-02	-6.28E-01	1.67E-01	3.67E-01	1.84E-01	6.96E-01	-3.02E-01	-6.31E-01
i = 8	1.63E-01	-7.49E-01	-5.72E-02	2.97E-01	-1.70E-01	5.15E-01	-3.04E-01	1.86E-01
i = 9	-2.68E-01	5.80E-01	-2.53E-01	-3.97E-01	-1.49E+00	-2.80E-01	1.85E-01	2.25E-01
i = 10	-3.69E-02	1.13E+00	-2.74E-02	4.50E-02	5.01E+00	-2.33E-01	-6.90E-02	-2.69E-02

j = 9	j = 10	j = 11	j = 12	j = 13	j = 14	j = 15	j = 16	j = 17	j = 18
-1.54E-01	-5.49E-01	6.72E-02	-1.51E-02	-2.07E-01	3.31E-02	3.03E-01	-6.46E-02	4.99E-01	-1.46E-01
-3.14E-01	-5.77E-01	4.80E-01	2.10E-01	5.30E-01	-1.39E-01	-7.90E-01	3.35E-01	5.91E-01	-4.32E-01
-2.79E-01	-5.97E-01	1.98E-01	1.73E-01	-4.37E-01	2.70E-01	1.32E+00	-7.27E-01	-3.47E-01	6.01E-01
-2.67E-01	-2.14E-02	8.60E-01	6.96E-01	-4.69E-02	3.59E-01	-8.68E-01	-3.75E-01	-1.91E-02	-1.32E-01
-7.47E-02	-7.71E-01	2.29E-02	-1.34E-01	1.39E+00	-4.29E-02	-5.56E-02	5.33E-02	1.66E-01	6.64E-03
-4.64E-02	-2.81E-01	2.73E-02	-9.49E-03	-2.38E+00	7.00E-03	5.85E-01	-6.93E-02	5.47E-02	-9.52E-01
8.93E-02	2.50E-01	1.02E-01	-1.13E-01	-1.08E+00	-2.19E-01	9.63E-02	3.65E-01	-7.85E-01	9.68E-01
-3.29E-01	1.07E+00	-5.58E-01	-9.24E-01	-4.58E-01	1.54E-01	7.88E-01	1.19E-01	5.02E-01	-1.26E-01
-2.08E-01	-1.24E+00	1.99E-01	-8.15E-02	4.09E-01	-1.28E-01	3.43E-01	1.84E-01	2.12E-01	4.09E-02
-3.71E-03	-2.62E-02	1.55E-02	-3.66E-02	7.76E-01	2.90E-02	-1.13E+00	1.72E-02	-5.92E-02	-1.12E+00

Table B2: Values of the weight matrix W_{ij}^2 for exceed absorptivity at P_gL ranging from 10 kPa-m to 50 kPa-m.

W_{ij}^3	j = 1	j = 2	j = 3	j = 4	j = 5
i = 1	-1.27E+00	-2.07E-01	-6.04E-01	-6.49E-02	-2.44E+00

j = 6	j = 7	j = 8	j = 9	j = 10
6.53E+00	-1.18E+00	-3.52E-03	1.03E+00	2.75E+00

Table B3: Values of the weight matrix W_{ij}^3 for exceed absorptivity at P_gL ranging from 10 kPa-m to 50 kPa-m.

b^1	i = 1	i = 2	i = 3	i = 4	i = 5	i = 6	i = 7	i = 8	i = 9
	-3.02E+00	1.45E+00	1.29E+00	-3.45E+00	-1.25E+01	-6.33E-01	-1.11E+00	-3.22E-01	4.70E-01

i = 10	i = 11	i = 12	i = 13	i = 14	i = 15	i = 16	i = 17	i = 18
1.18E-01	-1.42E-01	-4.98E-01	1.73E+00	2.46E+00	3.80E+00	2.83E+00	-1.79E+00	-2.79E+00

Table B4: Values of the bias vector b^1 for exceed absorptivity at P_gL ranging from 10 kPa-m to 50 kPa-m.

b^2	i = 1	i = 2	i = 3	i = 4	i = 5
	1.37E+00	1.53E+00	-1.02E+00	3.00E-01	6.46E-01

i = 6	i = 7	i = 8	i = 9	i = 10
-9.84E-01	2.18E-01	-1.03E+00	-1.62E+00	2.99E+00

Table B5: Values of the bias vector b^2 for exceed absorptivity at P_gL ranging from 10 kPa-m to 50 kPa-m.

b^3	i = 1
	1.12E-01

Table B6: Values of the bias vector b^3 for exceed absorptivity at P_gL ranging from 10 kPa-m to 50 kPa-m.

Appendix C: Expressions for Mass Conversion

The authors notice that mass for species and soot are typically being provided in fire safety/design calculations. In order to facilitate the radiation calculation, three expressions are presented below to convert 1) species mass for H_2O and CO_2 into partial pressure and 2) soot mass into soot volume fraction.

Assuming the total pressure of gaseous species to be 101.325 kPa, the partial pressure of H_2O can be obtained from the ideal gas law

$$P_{H_2O} = \frac{n_{H_2O} R T_g}{V}$$

where R is the universal gas constant (8.3143 J/mol/K or 8.20562e-5 atm·m^3/mol/K), T_g is the gas temperature (K), V is the volume of the mixture, and n_{H_2O} is the mole number of H_2O that can be evaluated by dividing the mass of H_2O by mole mass of H_2O

$$n_{H_2O} = \frac{m_{H_2O}}{M_{H_2O}}$$

for which the unit of m_{H_2O} and M_{H_2O} is kg and kg/mol, respectively. For H_2O, the mole mass is taken to be 18.0153e-3 kg/mol.Similarly, the partial pressure of CO_2 is given by

$$P_{CO_2} = \frac{m_{CO_2} R T_g}{M_{CO_2} V}$$

where the mole mass of CO_2 is taken to be 44.0088e-3 kg/mol. The soot volume fraction can be obtained from

$$f_v = \frac{m_{soot}}{V \rho_{soot}}$$

where m_{soot} is the mass of the soot and ρ_{soot} is the density of the soot that is taken to be 1800 kg/m^3.